Research Square

Preprints are preliminary reports that have not undergone peer review.
They should not be considered conclusive, used to inform clinical practice,
or referenced by the media as validated information.

Early Plasma Cytokine Profiling Refines Relapse Risk Beyond Interim Pet/Ct in Classical Hodgkin Lymphoma

Laura Gálvez-Carvajal
Hospital Clínico Universitario Virgen de la Victoria
Jesús Velasco-Suelto
Hospital Clínico Universitario Virgen de la Victoria
Silvia Sequero-López
University Hospital Clínico San Cecilio
Marcos Melián-Sosa
Fundación Instituto Valenciano de Oncología
Natividad Martínez-Banaclocha
Instituto de investigación sanitaria y biomédica de Alicante
María Casanova-Espinosa
Hospital Costa del Sol
Luis De la Cruz-Merino
Hospital Universitario Virgen Macarena
Natalia Palazón-Carrión
Hospital Universitario Virgen Macarena
Francisco Ramón García-Arroyo
Complejo Hospitalario de Pontevedra
Juan Daniel Prieto-Cuadra
Hospital Clínico Universitario Virgen de la Victoria
Maria Elena Quirós-Ortega
Hospital Clínico Universitario Virgen de la Victoria
Javier Pascual
Hospital Clínico Universitario Virgen de la Victoria
Mariano Provencio-Pulla
Hospital Universitario Puerta de Hierro Majadahonda
Rocío Lavado-Valenzuela
Hospital Clínico Universitario Virgen de la Victoria
Emilio Alba
Hospital Clínico Universitario Virgen de la Victoria
Antonio Rueda-Domínguez

Hospital Clínico Universitario Virgen de la Victoria

Iñaki Comino-Méndez

inaki.comino@ibima.eu

Hospital Clínico Universitario Virgen de la Victoria

Research Article

Keywords: Classical Hodgkin Lymphoma, cytokines, liquid biopsy, prognosis, tumor microenvironment (TME), interim PET/CT, longitudinal monitoring

Posted Date: July 20th, 2026

DOI: https://doi.org/10.21203/rs.3.rs-10347261/v1

License: This work is licensed under a Creative Commons Attribution 4.0 International License. Read Full License

Additional Declarations: No competing interests reported.

Abstract

Background

Classical Hodgkin lymphoma (cHL) is a microenvironment-driven malignancy in which soluble immune mediators may provide minimally invasive biomarkers of relapse risk beyond conventional clinical variables and interim PET/CT (iPET/CT).

Methods

We performed longitudinal plasma cytokine profiling of 30 cytokines in patients across baseline (T1), early on-treatment (T2) and after completion of therapy (T3/iPET/CT-aligned) to identify reproducible immune biomarkers associated with progression-free survival (PFS). Associations with progression-free survival (PFS) were assessed using differential expression, survival analyses, composite cytokine scores, and longitudinal trajectory modelling. Cytokine-derived biomarkers were also evaluated in combination with iPET/CT response.

Results

Baseline analyses showed that Eotaxin, MIP-1alpha, IL-6 and IL-2Ralpha differed between patients who later relapsed and those who remained relapse-free. Survival analyses identified Eotaxin, IL-6 and MCP-1 as prognostically relevant, with a baseline IL-6 + Eotaxin score providing the strongest baseline discrimination. At the early on-treatment timepoint (T2), several cytokines were associated with subsequent relapse, with the strongest signals observed for IL-7, IL-2Ralpha and Basic FGF. The T2 IL-7 + Basic FGF score yielded the best overall prognostic performance. In contrast, no significant differences were observed at the later T3/iPET/CT-aligned timepoint when absolute cytokine levels were considered. Longitudinal analyses identified IL-6 dynamics as the most consistent treatment-associated cytokine trajectory, with more pronounced IL-6 decreases from baseline associated with inferior PFS. In analyses integrating iPET/CT response, cytokine-derived biomarkers provided additional prognostic information. Among patients achieving CMR on iPET/CT, ΔIL-6 T1→T2 showed the strongest residual-risk stratification (HR per SD, 0.33; 95% CI, 0.15–0.75; p = 0.008; C-index, 0.72), while the T2 IL-7 + Basic FGF score was also associated with subsequent relapse (HR per SD, 2.49; 95% CI, 1.15–5.37; p = 0.020; C-index, 0.67).

Conclusions

Cytokine-derived biomarkers improved prognostic modelling beyond iPET/CT response and, importantly, retained prognostic value among patients achieving iPET/CT CMR, suggesting that early immune trajectories may reveal residual biological risk despite favorable metabolic imaging. These findings support multiplex plasma cytokine profiling as a discovery strategy to define biologically informed biomarkers that may complement PET-adapted risk stratification in cHL.

BACKGROUND

Classical Hodgkin lymphoma (cHL) is a B-cell–derived malignancy defined by the paradoxical coexistence of scarce malignant Hodgkin and Reed–Sternberg (HRS) cells and a disproportionately abundant, highly structured tumour microenvironment (TME). In most cases, HRS cells represent only a minor fraction of the cellular content of the involved tissue, yet they orchestrate a complex immune and stromal ecosystem through aberrant signalling programs and extensive cytokine/chemokine crosstalk. This biology underpins key clinical hallmarks of cHL, including systemic inflammatory symptoms, immune evasion, and the characteristic histopathological heterogeneity that forms the basis for recognised subtypes. Contemporary classifications continue to emphasise the centrality of microenvironmental context in defining disease entities and their clinicopathological correlates (1, 2).

Despite major therapeutic advances and high cure rates with first-line regimens, a clinically meaningful subset of patients experiences primary refractory disease or relapse. Current risk stratification relies heavily on clinical staging and response-adapted strategies, with ^{18}F-FDG PET/CT serving as the cornerstone for response assessment. Interim PET/CT (iPET/CT) after two cycles of chemotherapy is widely implemented to guide treatment escalation or de-escalation, reflecting its prognostic value across risk groups (3). However, PET/CT is not a perfect surrogate of residual viable disease. False-positive uptake related to treatment-induced inflammation, infection, or benign reactive processes may trigger unnecessary intensification, while false negatives may occur when residual disease burden falls below imaging resolution or exhibits altered metabolic behaviour. In addition, repeated imaging exposes patients, often adolescents and young adults, to cumulative ionising radiation, which is a non-trivial consideration for long-term survivorship (4). These limitations have fuelled interest in complementary biomarkers that capture tumour biology and host response with higher temporal resolution and lower burden for the patient (5, 6).

Liquid biopsy approaches have expanded the biomarker landscape in cHL, aiming to provide dynamic, minimally invasive readouts of disease activity. Among liquid biopsy analytes, soluble immune mediators are particularly compelling in cHL because the disease is fundamentally microenvironment-driven. Cytokines and chemokines mediate the bidirectional communication between HRS cells and surrounding immune/stromal compartments, shaping recruitment, activation, polarisation, and functional suppression of multiple cell types. The mechanistic relevance of cytokine signalling in cHL has long been recognised, with canonical work describing how cytokine networks contribute to the inflammatory phenotype and the distinctive cellular architecture of the TME (7). Importantly, these mediators are measurable in peripheral blood, raising the possibility of translating tumour–microenvironment biology into clinically actionable biomarkers (8–11). These observations motivate standardised longitudinal plasma profiling to complement PET-based response assessment. However, translation of cytokine biomarkers to routine care has been limited by methodological heterogeneity and inconsistent reproducibility across studies. In addition, most reports are cross-sectional, leaving early on-treatment immune dynamics insufficiently characterised

In this context, we analyzed plasma cytokines and chemokines across two complementary treatment-related time windows to characterize immune alterations in cHL and evaluate their association with relapse risk. By combining baseline profiling with both an early and a later on-treatment assessment, this strategy was designed to identify reproducible, quantitatively defined plasma biomarkers that may complement PET/CT and improve prognostication (Fig. 1A).

METHODS

Patients

Patients diagnosed with cHL were prospectively enrolled across the following participating institutions under institutionally approved protocols: Hospital Universitario Virgen de la Victoria, Instituto Valenciano de Oncología, Hospital Universitario San Cecilio, Hospital General Universitario Dr. Balmis, Hospital Universitario Virgen de la Macarena, Hospital Universitario Costa del Sol, Complejo Hospitalario de Pontevedra, and Hospital Universitario Puerta de Hierro Majadahonda. The study was conducted in accordance with the Declaration of Helsinki and was approved by the corresponding institutional or regional research ethics committees. Written informed consent was obtained from all participants before sample collection. The baseline clinicopathological characteristics of the study cohort are summarized in Table 1.

Table 1

Clinical characteristics of the study cohort. Summary of demographic and disease-related features for the 80 patients with classical Hodgkin lymphoma (cHL) included in the study. Data are presented as number of patients and percentage (%). *GHSG, German Hodgkin Study Group; Bulky disease, defined by Ann Arbor/Cotswold classification; IPS, International Prognostic Score; CMR: Complete Metabolic Response; PMR: Partial Metabolic Response.*

Characteristic	Overall (N = 80)	Non-relapse (N = 63)	Relapse (N = 17)
Clinical characteristics			
Age > 45 years	31/80 (38.8)	22/63 (34.9)	9/17 (52.9)
Female sex	43/80 (53.8)	33/63 (52.4)	10/17 (58.8)
Bulky disease	17/80 (21.3)	12/63 (19.0)	5/17 (29.4)
Extranodal involvement	32/80 (40.0)	22/63 (34.9)	10/17 (58.8)
Radiotherapy	9/80 (11.3)	8/63 (12.7)	1/17 (5.9)
GHSG risk group			
Initial	13/80 (16.3)	12/63 (19.0)	1/17 (5.9)
Intermediate	24/80 (30.0)	18/63 (28.6)	6/17 (35.3)
Advanced	43/80 (53.8)	33/63 (52.4)	10/17 (58.8)
Histological subtype			
Nodular sclerosis	54/73 (74.0)	39/57 (68.4)	15/16 (93.8)
Mixed cellularity	16/73 (21.9)	16/57 (28.1)	0/16 (0.0)
Lymphocyte-rich	2/73 (2.7)	2/57 (3.5)	0/16 (0.0)
Lymphocyte-depleted	1/73 (1.4)	0/57 (0.0)	1/16 (6.3)
Missing/unknown	7/80 (8.8)	6/63 (9.5)	1/17 (5.9)
Response assessment			
iPET/CT CMR	62/77 (80.5)	52/62 (83.9)	10/15 (66.7)
Missing	3/80 (3.8)	1/63 (1.6)	2/17 (11.8)
End-of-treatment PET CMR	63/73 (86.3)	56/59 (94.9)	7/14 (50.0)
Missing	7/80 (8.8)	4/63 (6.3)	3/17 (17.6)
Cytokine sample availability			
Baseline/T1 cytokines	79/80 (98.8)	62/63 (98.4)	17/17 (100.0)

Characteristic	Overall (N = 80)	Non-relapse (N = 63)	Relapse (N = 17)
Clinical characteristics			
Not available	1/80 (1.3)	1/63 (1.6)	0/17 (0.0)
Paired T1-T2 cytokines	38/80 (47.5)	22/63 (34.9)	16/17 (94.1)
Not available	42/80 (52.5)	41/63 (65.1)	1/17 (5.9)
Paired T1-T3 cytokines	71/80 (88.8)	57/63 (90.5)	14/17 (82.4)
Not available	9/80 (11.3)	6/63 (9.5)	3/17 (17.6)
All three timepoints	35/80 (43.8)	21/63 (33.3)	14/17 (82.4)
Not available	45/80 (56.3)	42/63 (66.7)	3/17 (17.6)

Blood collection and plasma processing

Blood samples venous blood was drawn and collected into CellSafe Preservative Tubes (Menarini Silicon Biosystems). Samples were centrifuged at 600 x g for 10 min, the supernatant (plasma) was collected and then another centrifuge at 5250 x g for 10 minutes. Then the supernatant was aliquoted and stored at -80°C until further analyses. Blood samples were collected at baseline before the first ABVD cycle (T1; n = 79), on day 29 before the second ABVD cycle in the paired T1–T2 subset (n = 38), and after the second ABVD cycle, before the third cycle and contemporaneous with iPET/CT assessment, in the paired T1–T3 subset (n = 71) (Fig. 1A).

Cytokine and Chemokine quantification

The concentrations of cytokines and chemokines in plasma samples were quantified according to the protocol provided by the Bio-Plex Pro™ Human Cytokine 27-plex Assay kit (Bio-Rad Laboratories, Hercules, CA, USA), complemented with single-analyte Bio-Plex assays for IL-2Ralpha (Bio-Plex Pro Human Cytokine IL-2Ralpha), HGF (Bio-Plex Pro Human Cytokine HGF) and MIG/CXCL9 (Bio-Plex Pro Human Cytokine MIG). Assay plates were read on a Bio-Plex® 200 System and analysed using Bio-Plex Manager™ MP software (Luminex, Austin, TX, USA) at the Proteomics Unit, Central Research Support Services, University of Málaga.

Analyte availability was not identical across all analytical subsets. HGF and MIG/CXCL9 were added to the expanded T1/T3 panel as additional single-analyte measurements, whereas the T1–T2 dataset was restricted to the core multiplex panel. Accordingly, these analytes were not included in early on-treatment analyses.

Data processing and derivation of longitudinal variables

Raw cytokine concentrations (pg/mL) were assembled into an analysis matrix and linked to clinical metadata. To reduce zero inflation arising from non-detectable measurements, analyte-specific replacement was applied only to cytokines exceeding the predefined frequency threshold for non-detectable values. For each cytokine, such values were replaced by the lowest measurable concentration for that analyte, defined as the minimum non-zero value observed for that cytokine in the dataset. Longitudinal change was quantified on the absolute concentration scale as Δ = post-baseline − T1 (pg/mL), considering both the T1→T2 and T1→T3 intervals.

To ensure technical robustness across analytical subsets, inter-kit comparability was assessed in paired T1 samples measured using two multiplex panels. Comparability was evaluated using Pearson and Spearman correlation coefficients, mean inter-kit difference, and mean absolute error (MAE). Analytes classified as having poor comparability or insufficient evaluability were excluded. Among analytes classified as having good comparability, those showing markedly greater absolute inter-kit disagreement than the rest of the retained panel were also excluded on pragmatic grounds. Using this strategy, IL-1ra, IP-10, and PDGF-BB, together with the cytokines classified with poor comparability, were not retained for downstream analyses.

Statistical analyses

Associations between cytokine levels and relapse status were assessed using two-sided Mann–Whitney U tests, with Benjamini–Hochberg false discovery rate correction applied within each timepoint-specific analysis. Univariable discrimination was summarised using the area under the receiver operating characteristic curve (AUC), and group medians were reported. Boxplots and paired box-and-slope plots were generated using raw concentration values to preserve biological interpretability.

Longitudinal change was defined on the absolute concentration scale as Δ = post-treatment (T2/T3) − T1 (pg/mL). Delta variables were analysed on their native scale for descriptive summaries and Kaplan–Meier stratification. Optimal cut-offs for Kaplan–Meier analyses were identified by maximising the log-rank statistic across candidate thresholds restricted to the 10th–90th percentiles of the marker distribution, requiring a minimum of 10 patients per group. Time-to-event associations for continuous predictors were evaluated using Cox proportional hazards regression. For continuous Cox models, predictors were internally standardised within each evaluable dataset so that hazard ratios (HRs) could be reported per 1 standard deviation (SD) increase. Thus, raw concentrations were used for descriptive, group-comparison, and Kaplan–Meier analyses, whereas internally standardised variables were used for continuous Cox modelling and multivariable cytokine combinations. Variables were analysed only when at least 10 evaluable samples and 5 events were available, and predictors with negligible variance or insufficient unique values were excluded. The proportional hazards assumption was assessed using a rank-based test of Schoenfeld residuals for each Cox model. Time-to-event analyses were performed within the corresponding evaluable subset after excluding patients without available follow-up time or

event status; accordingly, baseline, T1–T2 and T1–T3 survival analyses included 78, 38 and 70 patients, respectively.

To identify multivariable cytokine signatures, exhaustive searches of all 2- and 3-marker combinations were performed using ridge-penalised Cox regression (penalizer = 0.10). Predictors entering combination models were internally standardised before fitting, and linear predictor scores from the best-performing models were used for Kaplan–Meier visualisation.

Clinical variables were evaluated using univariable Cox proportional hazards regression. Models were fitted without penalization. Variables were analyzed only when at least 10 evaluable cases and 5 events were available. Models were fitted after excluding observations with missing time or event information. For each model, HRs, 95% confidence intervals, Wald p values, Benjamini–Hochberg q values, concordance index (C-index), and proportional hazards test p values were recorded.

To assess whether cytokine-derived biomarkers improved prognostic stratification beyond iPET/CT response, incremental Cox modelling was performed within each biomarker-specific complete-case subset. For each biomarker, a reference model including iPET/CT response alone was compared with an extended model including iPET/CT response plus the biomarker. Continuous cytokine-derived predictors were internally standardised before model fitting. Incremental prognostic value was quantified as the change in concordance index (ΔC-index) and formally assessed using likelihood-ratio tests for nested models. In a subsequent exploratory analysis restricted to patients achieving iPET/CT complete metabolic response (CMR), the baseline IL-6 + Eotaxin score, ΔIL-6 T1→T2, ΔIL-6 T1→T3, and the T2 IL-7 + Basic FGF score were evaluated for their ability to identify residual relapse risk. Within this subgroup, biomarker distributions were compared between patients who subsequently relapsed and those who remained relapse-free using Mann–Whitney U tests. Discrimination was summarized using AUC and oriented AUC, and time-to-event associations were assessed using continuous univariable Cox models with HRs reported per 1 standard deviation increase.

As a secondary analysis, baseline MIG/CXCL9 was assessed as a discriminator of histological subtype, comparing mixed cellularity versus nodular sclerosis cases. Group differences were evaluated using the Mann–Whitney U test, and classification performance was assessed using logistic regression with 30 repeats of 3-fold stratified cross-validation. Out-of-fold predictions were used to derive the ROC curve, AUC, average precision, and Brier score. The 95% confidence interval for the AUC was estimated by bootstrap resampling, and the optimal threshold was defined using Youden's index.

All analyses were performed in Python using standard scientific libraries, including pandas, numpy, scipy, scikit-learn, lifelines, matplotlib, and openpyxl, and were implemented through scripted workflows that generated the final result tables and publication-ready figures.

RESULTS

Baseline plasma cytokines associated with relapse

Baseline plasma cytokine levels (T1) were first evaluated in the technically retained analyte panel, which was defined after excluding cytokines with poor inter-kit comparability or insufficient evaluability in duplicated T1 samples measured using two different multiplex kits (**Supplementary Table S1**). In this context, Eotaxin, MIP-1alpha, IL-6, and IL-2Ralpha showed nominally significant baseline differences between patients who subsequently relapsed and those who remained relapse-free (**Fig. 1B** and **Supplementary Table S2**; Eotaxin, p = 0.028, AUC = 0.68; MIP-1alpha, p = 0.026, AUC = 0.68; IL-6, p = 0.048, AUC = 0.66; IL-2Ralpha, p = 0.048, AUC = 0.66).

Baseline survival analyses further supported the prognostic relevance of retained cytokines (**Fig. 1C**). Patients with high baseline Eotaxin levels had significantly shorter progression-free survival (PFS) than those with low levels (cutoff = 208; log-rank $p = 1.69 \times 10^{-6}$). A similar association was observed for IL-6 (cutoff = 4.48; log-rank p = 0.0132) and MCP-1 (cutoff = 39.2; log-rank p = 0.00511). Notably, the combined IL-6 + Eotaxin score provided the strongest baseline prognostic discrimination (cutoff = 0.525; log-rank $p = 1.55 \times 10^{-6}$), supporting the added value of multi-cytokine integration over individual baseline markers.

On-treatment cytokine profiles across the early and interim-response timepoints

At the T2 timepoint, corresponding to the early on-treatment window, several cytokines within the retained analyte panel showed significant differences between patients who later relapsed and those who remained relapse-free (**Fig. 2** and**Supplementary Table S3**). The strongest signal was observed for IL-7 ($p < 0.001$, q = 0.004, AUC = 0.83), followed by IL-2Ralpha (p = 0.003, q = 0.014, AUC = 0.78) and Basic FGF (p = 0.004, q = 0.014, AUC = 0.77). Additional significant differences were detected for IL-8 (p = 0.020, q = 0.033, AUC = 0.72), MIP-1alpha (p = 0.021, q = 0.033, AUC = 0.72), IL-1 beta (p = 0.021, q = 0.033, AUC = 0.72), and IL-4 (p = 0.023, q = 0.033, AUC = 0.72), while IL-6 also showed a weaker but still significant association (p = 0.041, q = 0.051, AUC = 0.68).

Among absolute T2 measurements, the combination of IL-7 and Basic FGF yielded the strongest prognostic model in the combination search, with a highly significant global likelihood ratio test in Cox regression (p global LR=0.000855, C-index=0.785). Dichotomisation of the derived score further showed marked outcome stratification (log-rank $p = 7.31 \times 10^{-8}$) (**Supplementary Fig. S1**).

In contrast, no cytokine within the retained analyte panel showed significant differences between outcome groups at end-of-treatment (T3) (**Supplementary Table S4**). Together, these findings indicate that the strongest treatment-associated plasma cytokine divergence linked to subsequent relapse is detectable early during therapy, whereas no clear separation in absolute cytokine levels is observed at the later timepoint.

IL-6 dynamics in treatment-associated prognostic signal

We next evaluated whether treatment-associated cytokine changes from baseline were associated with PFS by analyzing ΔT1→T2 and ΔT1→T3 values across the retained cytokine panel. Across these

analyses, ΔIL-6 emerged as the most consistent dynamic biomarker. It was the only cytokine that showed significant associations with outcome in continuous univariable Cox models at both longitudinal intervals, for both ΔIL-6 (T2−T1) (HR per SD = 0.61, 95% CI 0.42–0.88; p = 0.0075; C-index = 0.612; PH test p = 0.667) and ΔIL-6 (T3−T1) (HR per SD = 0.68, 95% CI 0.48–0.94; p = 0.0216; C-index = 0.660; PH test p = 0.363) (**Supplementary Table S5**). By contrast, other cytokines showed survival separation only in cutpoint-based analyses and were therefore interpreted more cautiously. In the ΔT1→T2 analysis, ΔMCP-1 (log-rank p = 0.0140; HR 0.38, 95% CI 0.15–0.93) and ΔIL-8 (log-rank p = 0.0328; HR 2.37, 95% CI 0.96–5.88) also showed outcome stratification. In the ΔT1→T3 analysis, ΔMCP-1 (log-rank p = 0.0116; HR 0.37, 95% CI 0.14–1.01), ΔBasic FGF (log-rank p = 0.0252; HR 0.42, 95% CI 0.17–1.08), ΔIL-7 (log-rank p = 0.0292; HR 0.45, 95% CI 0.19–1.11), and ΔIL-2Ralpha (log-rank p = 0.0331; HR 0.43, 95% CI 0.16–1.15) showed significant survival separation, but none demonstrated the same level of consistency across both dynamic windows as ΔIL-6 (**Supplementary Table S6** and **Supplementary Fig. S2**).

On this basis, we selected IL-6 for focused visualization of its paired longitudinal behavior within relapse and non-relapse groups. IL-6 concentrations changed significantly from T1 to T2 in both non-relapsing patients (paired Wilcoxon p = 0.0214) and relapsing patients (p = 0.0034) (**Fig. 3A**). A similar pattern was observed from T1 to T3, with significant within-group changes in both non-relapsing (p = 0.0007) and relapsing patients (p = 0.0058) (**Fig. 3B**), indicating that IL-6 undergoes treatment-associated modulation in both outcome groups.

Consistently, cutpoint-based survival analysis identified a threshold of −9.54 for ΔIL-6 (T2−T1), with patients showing higher delta values experiencing significantly better PFS than those with more negative changes (log-rank p = 0.0064; HR = 0.34, 95% CI 0.14–0.85; p = 0.0207) (**Fig. 3C**). Likewise, a cutpoint of −7.42 for ΔIL-6 (T3−T1) separated patients with significantly different outcomes (log-rank p = 0.0094; HR = 0.38, 95% CI 0.15–0.98; p = 0.0449) (**Fig. 3D**). Together, these results indicate that patients with a more pronounced decrease in IL-6 from baseline had inferior PFS, both early during treatment and at the later timepoint.

Integrated prognostic performance of cytokine-based and clinical models

To compare the prognostic relevance of cytokine-derived markers with standard clinical variables, we next examined both univariate Cox associations with PFS and global discriminative performance across the main candidate biomarkers identified in the previous analyses (**Fig. 4A**). In univariate Cox models, several cytokines showed significant associations with outcome, including Eotaxin (T1) (HR=2.02, 95% CI 1.35–3.02; p=0.001), MCP-1 (T1) (HR=1.69, 95% CI 1.11–2.60; p=0.015), and IL-6 (T1) (HR=1.55, 95% CI 1.15–2.08; p=0.004). Among on-treatment markers measured at T2, Basic FGF (HR=2.45, 95% CI 1.37–4.41; p=0.003), IL-7 (HR=2.31, 95% CI 1.56–3.42; p<0.001), IL-1 beta (HR=2.12, 95% CI 1.30–3.46; p=0.003), IL-4 (HR=2.07, 95% CI 1.27–3.36; p=0.004), IL-6 (HR=1.55, 95% CI 1.16–2.08; p=0.003), and IL-2Ralpha (HR=1.62, 95% CI 1.08–2.42; p=0.018) were also significantly associated with shorter PFS. By contrast, none of the clinical variables reached statistical significance. The strongest nominal associations were observed for iPET/CT response (Partial molecular response (PMR) vs Complete

molecular response (CMR): HR=2.62, 95% CI 0.90–7.68, p=0.079) and histological subtype—nodular sclerosis (HR=5.75, 95% CI 0.76–43.58, p=0.090) (**Supplementary Table S7**).

We then compared the discriminative performance of the main cytokine-based models against individual clinical variables using the concordance index (C-index) **(Fig. 4B)**. The T2 cytokine combination score based on IL-7 and Basic FGF showed the strongest performance overall (C-index=0.785), followed by the T1 IL-6 + Eotaxin score (C-index=0.714). The dynamic IL-6-derived markers also retained prognostic value, with ΔIL-6 T1→T3 reaching a C-index of 0.660 and ΔIL-6 T1→T2 a C-index of 0.612. Among clinical variables, the highest discrimination was observed for extranodal involvement (C-index=0.609) and histology—nodular sclerosis (C-index=0.605). Overall, these analyses indicate that cytokine-based models, particularly the T2 IL-7 + Basic FGF score and the T1 IL-6 + Eotaxin score, provided stronger prognostic discrimination than any individual clinical variable (**Supplementary Table S7 and S8**).

We next examined whether selected cytokine-derived biomarkers added prognostic information beyond iPET/CT response. Addition of the T2 IL-7 + Basic FGF score provided the greatest improvement in discrimination (ΔC-index = 0.141; LR p = 0.001). Both ΔIL-6 T1→T2 (ΔC-index = 0.121; LR p = 0.006) and ΔIL-6 T1→T3 (ΔC-index = 0.101; LR p = 0.026) were also associated with incremental prognostic gain. The baseline IL-6 + Eotaxin score showed a more modest but still significant improvement over PET2 (ΔC-index = 0.078; LR p = 0.006) (**Fig. 4C and Supplementary Table S9**). These findings support a complementary role for cytokine-derived biomarkers in refining risk stratification.

We finally performed an exploratory subgroup analysis restricted to patients achieving iPET/CT complete metabolic response (CMR), comparing those who subsequently relapsed with those who remained relapse-free, to determine whether cytokine-derived biomarkers could identify residual relapse risk within this apparently favorable metabolic-response group (**Fig. 4D**). Within the iPET/CT-CMR subgroup, ΔIL-6 T1→T2 showed the strongest overall performance, with the highest discriminatory accuracy (oriented AUC = 0.735) and the highest Cox-based prognostic performance (HR per SD = 0.33, 95% CI 0.15–0.75; p = 0.008; C-index = 0.721). The T2 IL-7 + Basic FGF score showed very similar discrimination (oriented AUC = 0.733) and also remained associated with subsequent relapse in continuous Cox analysis (HR per SD = 2.49, 95% CI 1.15–5.37; p = 0.020; C-index = 0.673). ΔIL-6 T1→T3 retained prognostic value within iPET/CT-CMR patients (HR per SD = 0.50, 95% CI 0.30–0.84; p = 0.009; C-index = 0.652; oriented AUC = 0.639), whereas the baseline IL-6 + Eotaxin score showed a weaker but still significant association (HR per SD = 1.80, 95% CI 1.03–3.15; p = 0.040; C-index = 0.582; oriented AUC = 0.582) (**Supplementary Table S10**). Together, these findings suggest that dynamic and early on-treatment cytokine biomarkers may reveal residual risk even among patients classified as PET2-CMR.

Baseline MIG/CXCL9 discriminates histological subtype

We next explored whether baseline cytokine profiling also captured biological differences across histological subtypes. In this secondary analysis, baseline MIG/CXCL9 discriminated mixed cellularity (MC) from nodular sclerosis (NS) histology. MIG/CXCL9 levels were significantly higher in MC than in NS cases (median 1653.16 vs 231.84; Mann–Whitney $p = 3.2 \times 10^{-5}$). In a logistic regression model

evaluated using 30 repeats of 3-fold stratified cross-validation, the out-of-fold ROC analysis yielded an AUC of 0.79 (95% CI 0.62–0.94 by bootstrap resampling). The threshold selected by Youden's index was 0.25, corresponding to 75% sensitivity and 89% specificity (**Supplementary Fig. S3**).

DISCUSSION

cHL is a microenvironment-driven malignancy in which circulating cytokines may provide a minimally invasive readout of tumor–host interactions not fully captured by PET/CT or conventional clinical variables(2, 7). In this study, longitudinal plasma profiling identified complementary prognostic layers, a baseline IL-6 + Eotaxin score (T1), an early on-treatment IL-7 + Basic FGF score (T2), and dynamic IL-6 trajectories. Importantly, these biomarkers added prognostic information beyond iPET/CT and retained value among patients achieving iPET/CT CMR, suggesting that cytokine profiling may help identify residual biological risk despite favorable interim metabolic imaging.

Previous studies have established the prognostic relevance of soluble immune mediators in cHL, especially at diagnosis. Casasnovas et al. showed that pretreatment IL1-RA, IL-6 and soluble CD30 defined an outcome-associated plasma signature, while Marri et al. identified IL-6 and soluble IL-2Ralpha as among the most informative pretreatment cytokines(10, 12). Our findings are consistent with this literature, as both cytokines were associated with relapse. However, our data extend previous baseline-focused studies by showing that IL-6 gained prognostic value when integrated with Eotaxin and that IL-6 dynamics during therapy were consistently associated with PFS. Eotaxin/CCL11 is biologically plausible in cHL, as HRS cells can induce fibroblast-derived Eotaxin secretion, and Eotaxin expression has been linked to tissue eosinophilia(13, 14). Thus, the IL-6 + Eotaxin score may reflect a tumor-supportive inflammatory and eosinophil/Th2-oriented microenvironment rather than effective antitumor immunity.

A distinctive observation was that the strongest relapse-associated cytokine divergence appeared at T2, after the first treatment cycle, whereas no retained cytokine differed significantly at the later T3/iPET/CT-aligned timepoint. This suggests that immune divergence may emerge early and may not be fully captured at blood iPET/CT timepoint. This concept is related to previous work on TARC/CCL17, the most extensively studied soluble biomarker in cHL(15–17). Guidetti et al. showed that early TARC reduction after one ABVD cycle was associated with iPET/CT negativity and favorable outcome(18). Our study extends this early-response paradigm beyond a single chemokine by showing that multiplex cytokine profiling can identify early relapse-associated immune signatures. Among these, the IL-7 + Basic FGF score showed the strongest discriminative performance. IL-7 has direct biological relevance in cHL through IL-7/IL-7R signaling in HRS cells, whereas Basic FGF may reflect stromal remodeling or angiogenic repair programs during therapy(19).

The dynamic IL-6 findings add an additional layer of information. High baseline IL-6 was associated with adverse outcome, in line with previous studies(10, 12), while more pronounced IL-6 decreases during treatment also predicted inferior PFS. These findings are not necessarily contradictory, baseline IL-6 likely reflects inflammatory tumor burden, whereas IL-6 kinetics may capture treatment-induced immune

reconfiguration. The fact that ΔIL-6 was significant across both longitudinal windows supports its interpretation as the most consistent treatment-associated cytokine trajectory in this dataset.

Clinically, one of the most relevant finding is that cytokine biomarkers refined risk beyond iPET/CT. iPET/CT-CMR identifies a favorable group, but some patients still relapse. In our iPET-CMR subgroup, dynamic IL-6 and the T2 IL-7 + Basic FGF score identified residual relapse risk despite CMR. This is conceptually aligned with the HD0607 TARC substudy, where elevated TARC after two ABVD cycles predicted inferior PFS even among iPET/CT-negative patients(11), and with the SWOG S0816 correlative study, where soluble immune mediators provided prognostic information alongside PET response(20). Therefore, cytokine profiling should not be viewed as a replacement for PET/CT, but as a complementary biological layer that may resolve heterogeneity among metabolically responding patients.

This study has limitations. The sample size and number of relapse events were limited, particularly for subgroup analyses and for the paired T1–T2 dataset. In addition, cytokine availability differed across analytical subsets, and technical filtering, although important to improve robustness, reduced the number of analytes evaluated. The cytokine combinations and cutpoint-based Kaplan–Meier thresholds were data-driven and should therefore be considered exploratory until externally validated in independent cohorts. Finally, plasma cytokine measurements cannot define the cellular source or mechanistic basis of the observed immune trajectories.

CONCLUSIONS

Longitudinal plasma cytokine profiling identified biologically informative immune biomarkers associated with relapse risk in cHL. In particular, baseline and early on-treatment cytokine scores provided the strongest prognostic discrimination, while cytokine-derived biomarkers retained prognostic value even among patients achieving complete metabolic response, indicating that circulating immune signals capture residual biological risk beyond metabolic imaging alone. These findings support plasma cytokine profiling as a minimally invasive strategy to refine PET-adapted risk stratification and provide a rationale for the prospective validation of immune-based biomarkers in personalized disease monitoring.

Abbreviations

cHL: Classical Hodgkin lymphoma

PET/CT: Positron emission tomography/computed tomography

iPET/CT: Interim PET/CT

PFS: Progression-free survival

HRS: Hodgkin and Reed–Sternberg

TME: Tumor microenvironment

18F-FDG Fluorine-18 fluorodeoxyglucose

TARC: Thymus and activation-regulated chemokine

CMR: Complete metabolic response

ABVD: Doxorubicin, Bleomycin, Vinblastine and Dacarbazine

NS: Nodular sclerosis

MC: Mixed cellularity

ROC: Receiver operating characteristic

AUC: Area under the curve

HR: Hazard ratio

CI: Confidence interval.

Declarations

Ethics approval and consent to participate

Written informed consent was obtained from all participants prior to sample collection. The study was approved by the Comité de Ética de la Investigación Provincial de Málaga and conducted in accordance with the Declaration of Helsinki and all applicable national and institutional regulations.

Consent for publication

Not applicable.

Availability of data and materials

All data generated or analysed during this study are included in this published article and its supplementary information files. The plasma cytokine concentration dataset generated during the current study is publicly available in Zenodo at https://doi.org/10.5281/zenodo.21276553.

Competing interests

The authors declare that they have no competing interests

Funding

This study was partially funded by a research grant from the Sociedad Andaluza de Oncología Médica (SAOM) awarded to Dr Laura Gálvez-Carvajal, the Grupo Oncológico para el Tratamiento y Estudio de los

Linfomas (GOTEL), and institutional support from the Biomedical Research Institute of Málaga (IBIMA Plataforma BIONAND) awarded to Dr Iñaki Comino-Méndez.

Authors' contributions

I.C.M., J.V.S. and M.E.Q.O designed and performed experiments. L.G.C. coordinated patient recruitment and sample logistics, in collaboration with S.S.L., M.M.S., N.M.B., M.C.E., L.C.M., N.P.C., F.R.G.A., J.D.P.C., J.P., M.P.P., A.R.D., R.L.V., and E.A.. I.C.M. and A.R.D. jointly supervised the study as senior authors. All authors contributed to data interpretation, critically revised the manuscript, approved the final version, and consented to its publication.

Acknowledgements

We are deeply grateful to the patients and their families for their participation and trust. We thank the clinical staff and research teams at Hospital Universitario Virgen de la Victoria for their continuous support, and particularly the Medical Oncology Unit at Hospital Universitario Virgen de la Victoria for facilitating the development of this project. We also acknowledge the technical assistance provided by the Laboratorio de Biología Molecular del Cáncer (LBMC)/CIMES. Funding for Dr Iñaki Comino-Méndez contract was provided by the Spanish Government through the Ramón y Cajal Grant RYC2023-044581-I, funded by MICIU/AEI /10.13039/501100011033 and co-financed by the European Social Fund Plus (FSE+).

References

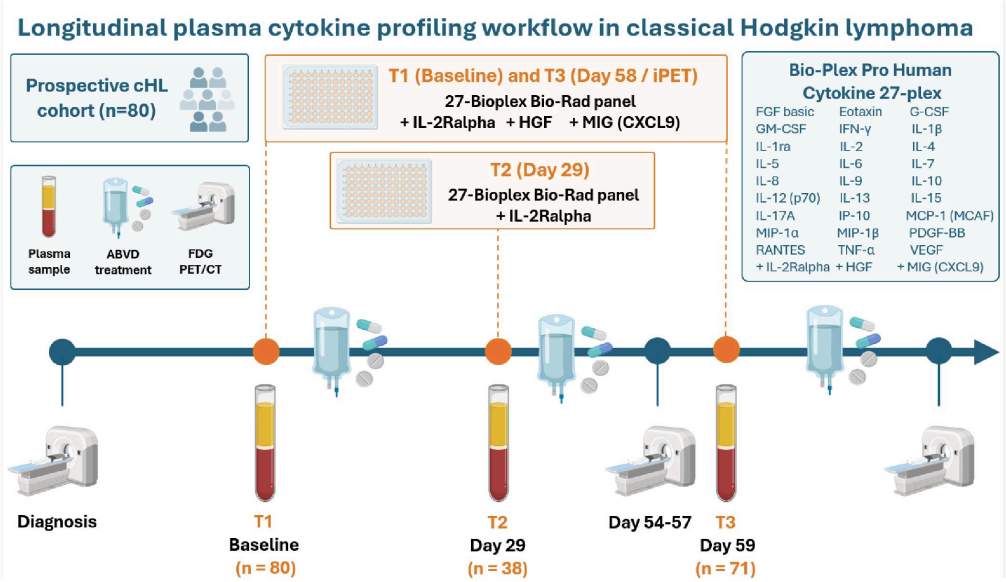
1. Medeiros LJ, Chadburn A, Natkunam Y, Naresh KN, Project WHOtEC. Fifth Edition of the World Health Classification of Tumors of the Hematopoietic and Lymphoid Tissues: B-cell Neoplasms. Mod Pathol. 2024;37(4):100441.
2. Weniger MA, Küppers R. Molecular biology of Hodgkin lymphoma. Leukemia. 2021;35(4):968–81.
3. de Wit M, Bohuslavizki KH, Buchert R, Bumann D, Clausen M, Hossfeld DK. 18FDG-PET following treatment as valid predictor for disease-free survival in Hodgkin's lymphoma. Ann Oncol. 2001;12(1):29–37.
4. Goldschmidt N, Or O, Klein M, Savitsky B, Paltiel O. The role of routine imaging procedures in the detection of relapse of patients with Hodgkin lymphoma and aggressive non-Hodgkin lymphoma. Ann Hematol. 2011;90(2):165–71.
5. Ansell SM. Hodgkin lymphoma: 2025 update on diagnosis, risk-stratification, and management. Am J Hematol. 2024;99(12):2367–78.
6. Velasco-Suelto J, Gálvez-Carvajal L, Comino-Méndez I, Rueda-Domínguez A. Hodgkin lymphoma and liquid biopsy: a story to be told. J experimental Clin cancer research: CR. 2024;43(1):184.
7. Skinnider BF, Mak TW. The role of cytokines in classical Hodgkin lymphoma. Blood. 2002;99(12):4283–97.

8. Agrusa JE, Scull BP, Abhyankar HA, Lin H, Ozuah NW, Chakraborty R et al. Defining the Inflammatory Plasma Proteome in Pediatric Hodgkin Lymphoma. Cancers. 2020;12(12).
9. Levin LI, Breen EC, Birmann BM, Batista JL, Magpantay LI, Li Y, et al. Elevated Serum Levels of sCD30 and IL6 and Detectable IL10 Precede Classical Hodgkin Lymphoma Diagnosis. Cancer Epidemiol Biomarkers Prev. 2017;26(7):1114–23.
10. Marri PR, Hodge LS, Maurer MJ, Ziesmer SC, Slager SL, Habermann TM, et al. Prognostic significance of pretreatment serum cytokines in classical Hodgkin lymphoma. Clin cancer research: official J Am Association Cancer Res. 2013;19(24):6812–9.
11. Viviani S, Mazzocchi A, Pavoni C, Taverna F, Rossi A, Patti C, et al. Early serum TARC reduction predicts prognosis in advanced-stage Hodgkin lymphoma patients treated with a PET-adapted strategy. Hematol Oncol. 2020;38(4):501–8.
12. Casasnovas RO, Mounier N, Brice P, Divine M, Morschhauser F, Gabarre J, et al. Plasma cytokine and soluble receptor signature predicts outcome of patients with classical Hodgkin's lymphoma: a study from the Groupe d'Etude des Lymphomes de l'Adulte. J Clin Oncol. 2007;25(13):1732–40.
13. Jundt F, Anagnostopoulos I, Bommert K, Emmerich F, Müller G, Foss HD, et al. Hodgkin/Reed-Sternberg cells induce fibroblasts to secrete eotaxin, a potent chemoattractant for T cells and eosinophils. Blood. 1999;94(6):2065–71.
14. Teruya-Feldstein J, Jaffe ES, Burd PR, Kingma DW, Setsuda JE, Tosato G. Differential chemokine expression in tissues involved by Hodgkin's disease: direct correlation of eotaxin expression and tissue eosinophilia. Blood. 1999;93(8):2463–70.
15. Jones K, Vari F, Keane C, Crooks P, Nourse JP, Seymour LA, et al. Serum CD163 and TARC as disease response biomarkers in classical Hodgkin lymphoma. Clin Cancer Res. 2013;19(3):731–42.
16. Plattel WJ, van den Berg A, Visser L, van der Graaf AM, Pruim J, Vos H, et al. Plasma thymus and activation-regulated chemokine as an early response marker in classical Hodgkin's lymphoma. Haematologica. 2012;97(3):410–5.
17. Zijtregtop EAM, van der Strate I, Beishuizen A, Zwaan CM, Scheijde-Vermeulen MA, Brandsma AM et al. Biology and Clinical Applicability of Plasma Thymus and Activation-Regulated Chemokine (TARC) in Classical Hodgkin Lymphoma. Cancers (Basel). 2021;13(4).
18. Guidetti A, Mazzocchi A, Miceli R, Paterno E, Taverna F, Spina F, et al. Early reduction of serum TARC levels may predict for success of ABVD as frontline treatment in patients with Hodgkin Lymphoma. Leuk Res. 2017;62:91–7.
19. Cattaruzza L, Gloghini A, Olivo K, Di Francia R, Lorenzon D, De Filippi R, et al. Functional coexpression of Interleukin (IL)-7 and its receptor (IL-7R) on Hodgkin and Reed-Sternberg cells: Involvement of IL-7 in tumor cell growth and microenvironmental interactions of Hodgkin's lymphoma. Int J Cancer. 2009;125(5):1092–101.
20. Hsi ED, Li H, Nixon AB, Schoder H, Bartlett NL, LeBlanc M, et al. Serum levels of TARC, MDC, IL-10, and soluble CD163 in Hodgkin lymphoma: a SWOG S0816 correlative study. Blood. 2019;133(16):1762–5.

Figures

Fig. 1

A



B **C**

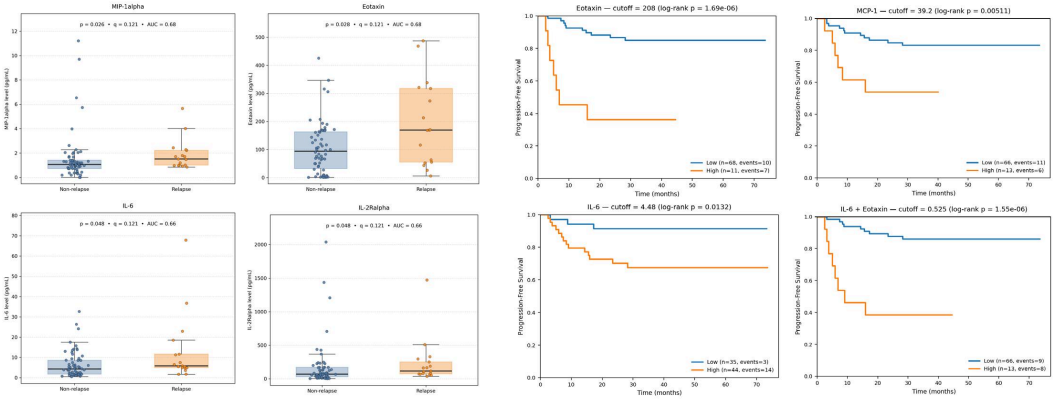


Figure 1

Longitudinal plasma cytokine profiling workflow and baseline plasma cytokines associated with relapse and progression-free survival in cHL. (A) Schematic overview of the longitudinal plasma cytokine profiling workflow. **(B)** Boxplots showing baseline (T1) plasma cytokine levels in patients who

remained relapse-free (blue) and in patients who later relapsed (orange) within the technically retained analyte panel. Each dot represents one individual patient. Boxes indicate the interquartile range (IQR), the horizontal line represents the median, and whiskers extend to 1.5×IQR. Shown are the retained baseline cytokines with nominally significant differences between outcome groups. **(C)**Kaplan–Meier progression-free survival curves according to baseline cytokine levels or combined baseline cytokine score. Cutoffs were determined by maximization of the log-rank statistic. Numbers in the legend indicate the number of patients and events in each group.

Fig. 2

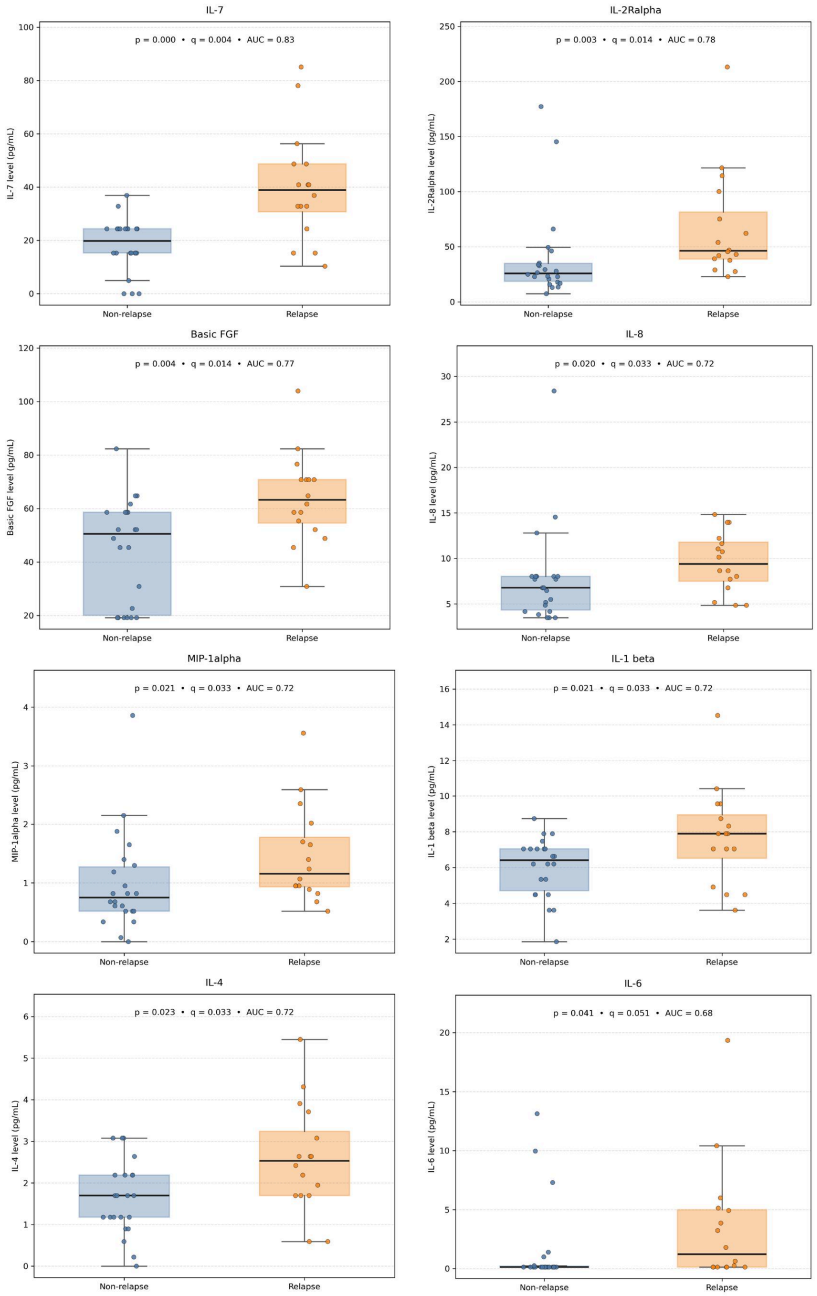


Figure 2

Early on-treatment plasma cytokines associated with subsequent relapse at T2. Boxplots showing plasma cytokine levels at the T2 timepoint in patients who remained relapse-free (blue) and in patients who later relapsed (orange). Each dot represents one individual patient. Boxes indicate the interquartile range (IQR), the horizontal line represents the median, and whiskers extend to 1.5×IQR. Shown are the T2 cytokines with significant differences between outcome groups within the retained analyte panel.

Fig. 3

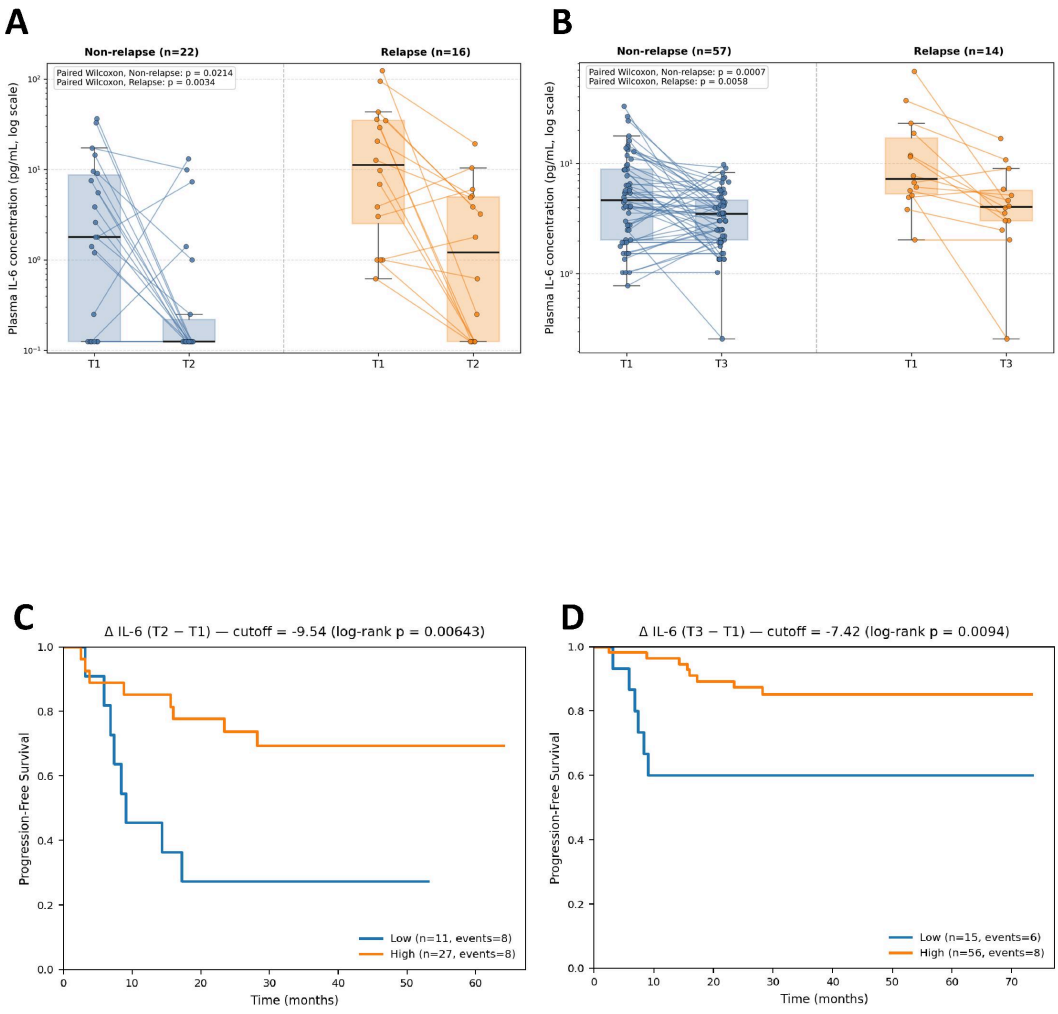


Figure 3

IL-6 treatment-associated dynamics are associated with progression-free survival. (A) Paired box-and-slope plot showing plasma IL-6 levels at T1 and T2 in non-relapsing and relapsing patients. Each line represents one patient, and paired Wilcoxon tests were used to assess within-group changes. **(B)** Kaplan–Meier progression-free survival curves according to ΔIL-6 (T2−T1). Cutoff-based analysis identified a threshold of −9.54, with more negative early IL-6 changes associated with inferior progression-free survival (log-rank p = 0.0064). **(C)** Paired box-and-slope plot showing plasma IL-6 levels at T1 and T3 in non-relapsing and relapsing patients. **(D)** Kaplan–Meier progression-free survival curves according to ΔIL-6 (T3−T1). A cutoff of −7.42 also separated patients with significantly different outcomes (log-rank p = 0.0106), indicating that more pronounced reductions in IL-6 from baseline were associated with shorter progression-free survival.

Fig. 4

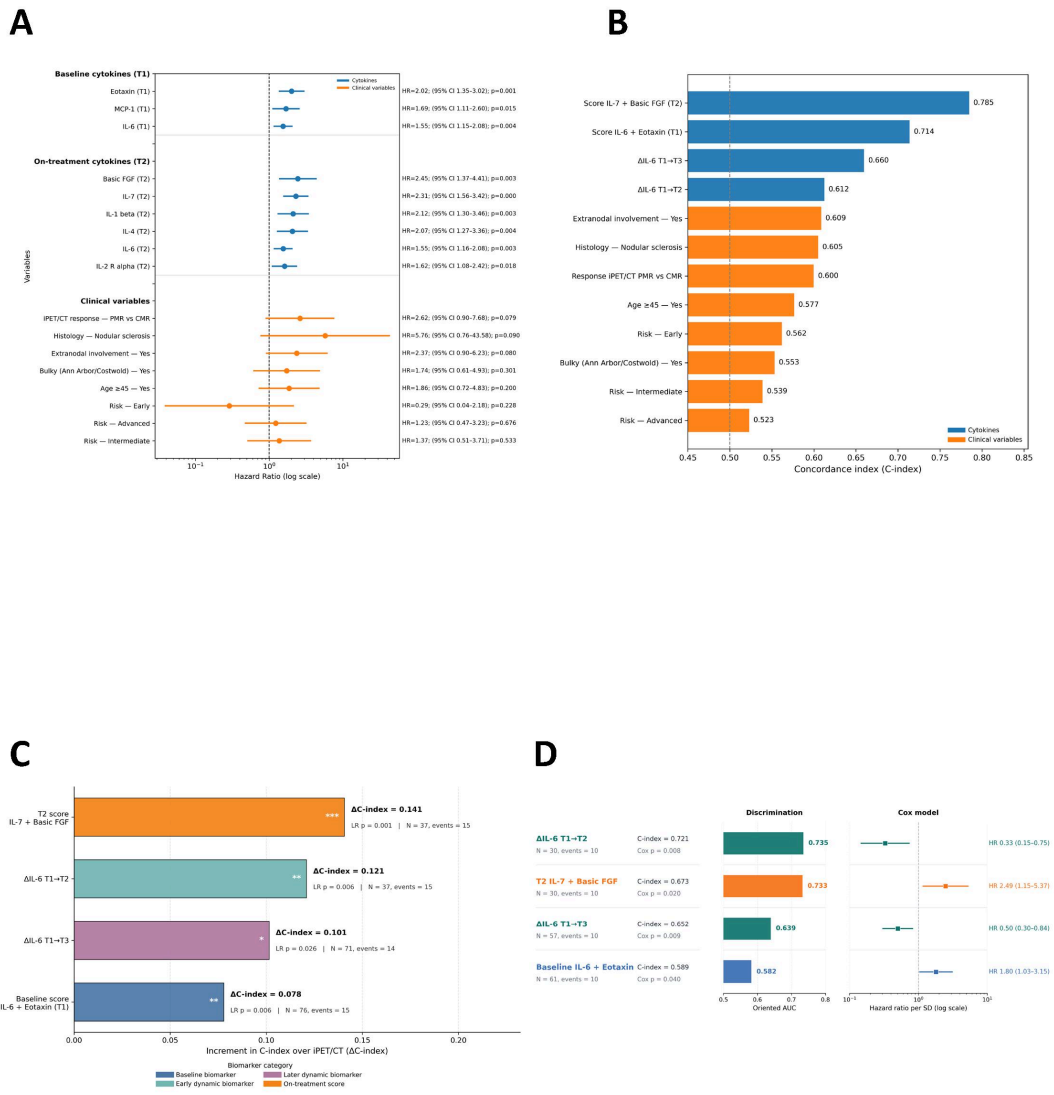


Figure 4

Integrated prognostic performance of cytokine-based and clinical models. (A) Univariate Cox analysis of selected cytokine and clinical predictors of progression-free survival. Baseline cytokines (T1), on-treatment cytokines (T2), and clinical variables are shown with hazard ratios (HRs), 95% confidence intervals, and p values. The dashed vertical line indicates HR=1. **(B)**Comparative discriminative performance of selected cytokine-based and clinical models assessed by the concordance index (C-

index). Cytokine-derived models included the baseline IL-6 + Eotaxin score (T1), ΔIL-6 T1→T2, ΔIL-6 T1→T3, and the T2 IL-7 + Basic FGF score. Clinical variables are shown individually for comparison. The dashed vertical line indicates a C-index of 0.50, corresponding to non-informative discrimination. **(C)** Incremental prognostic gain over iPET/CT-CMR provided by selected cytokine-derived biomarkers. Bars represent the increase in concordance index (ΔC-index) after adding each biomarker to iPET/CT. P values correspond to nested likelihood-ratio tests comparing iPET/CT alone versus iPET/CT plus biomarker within each evaluable subcohort. **(D)**Exploratory subgroup analysis restricted to patients achieving iPET/CT complete metabolic response (CMR). Selected cytokine-derived biomarkers were evaluated for their ability to identify residual relapse risk within this apparently favorable subgroup. The left panel shows the C-index and p value for each biomarker, together with the corresponding sample size and number of events. The middle panel shows the oriented AUC for discrimination between patients with and without subsequent relapse. The right panel displays hazard ratios (HRs) per 1 standard deviation increase with 95% confidence intervals from continuous univariable Cox models.

Supplementary Files

This is a list of supplementary files associated with this preprint. Click to download.

- SupplementaryTablesv3.xlsx
- SupplementaryFiguresv3.pdf